



Published in final edited form as:

*Ophthalmology*. 2019 January ; 126(1): 38–48. doi:10.1016/j.ophtha.2018.10.031.

## Genetic Architecture of Primary Open Angle Glaucoma in Individuals of African Descent: The African Descent & Glaucoma Evaluation Study (ADAGES) III

Kent D. Taylor, PhD<sup>#1</sup>, Xiuqing Guo, PhD<sup>#1</sup>, Linda M. Zangwill, PhD<sup>2</sup>, Jeffrey M. Liebmann, MD<sup>3</sup>, Christopher A. Girkin, MD<sup>4</sup>, Robert M. Feldman, MD<sup>5</sup>, Harvey Dubiner, MD<sup>6</sup>, Yang Hai<sup>\*\*1</sup>, Brian C. Samuels, MD, PhD<sup>4</sup>, Joseph F. Panarelli, MD<sup>13</sup>, John P. Mitchell, MD<sup>3</sup>, Lama A. Al-Aswad, MD<sup>5</sup>, Sung Chul Park, MD<sup>13</sup>, Celso Tello, MD<sup>13</sup>, Jeremy Cotliar, MD<sup>3</sup>, Rajendra Bansal, MD<sup>3</sup>, Paul A. Sidoti, MD<sup>13</sup>, George A. Cioffi, MD<sup>3</sup>, Dana Blumberg, MD<sup>3</sup>, Robert Ritch, MD<sup>13</sup>, Nicholas P. Bell, MD<sup>5</sup>, Lauren S. Blieden, MD<sup>5</sup>, Garvin Davis, MD<sup>5</sup>, Felipe A. Medeiros, MD, PhD<sup>2</sup>, Swapan K. Das, PhD<sup>8,9</sup>, Jasmin Divers, PhD<sup>7,12</sup>, Carl D. Langefeld, PhD<sup>8,12</sup>, Nicholette D. Palmer, PhD<sup>7,8,10,12</sup>, Barry I. Freedman, MD<sup>8,9,11</sup>, Donald W. Bowden, PhD<sup>7,10,11</sup>, Maggie C. Y. Ng, PhD<sup>7,10,11</sup>, Yii-Der Ida Chen, PhD<sup>1</sup>, Radha Ayyagari, PhD<sup>2</sup>, Jerome I. Rotter, MD<sup>1</sup>, Robert N. Weinreb, MD<sup>2</sup>, and ADAGES III Genomics Study Group

<sup>1</sup>Institute for Translational Genomics and Population Sciences and Department of Pediatrics, Los Angeles Biomedical Research Institute at Harbor-UCLA Medical Center, Torrance, California.

<sup>2</sup>Department of Ophthalmology, Hamilton Glaucoma Center, Shiley Eye Institute, University of California, San Diego, La Jolla, California.

<sup>3</sup>Bernard and Shirlee Brown Glaucoma Research Laboratory, Harkness Eye Institute, Columbia University Medical Center, New York, New York.

<sup>4</sup>Department of Ophthalmology, University of Alabama at Birmingham, Birmingham, Alabama.

<sup>5</sup>Ruiz Department of Ophthalmology and Visual Science, McGovern Medical School, The University of Texas Health Science Center at Houston, Houston, Texas.

Mailing Address: Robert N. Weinreb MD, University of California, San Diego, 9500 Gilman Drive, La Jolla, CA 92093-0946, rweinreb@ucsd.edu.

<sup>\*\*</sup>Current address: Department of Statistics, University of Auckland, Auckland, New Zealand.

**Publisher's Disclaimer:** This is a PDF file of an unedited manuscript that has been accepted for publication. As a service to our customers we are providing this early version of the manuscript. The manuscript will undergo copyediting, typesetting, and review of the resulting proof before it is published in its final citable form. Please note that during the production process errors may be discovered which could affect the content, and all legal disclaimers that apply to the journal pertain.

Conflict of Interest

KDT: none

XG: none

LMZ: Carl Zeiss Meditec, Heidelberg Engineering, Optovue Inc., Topcon Medical System Inc. (financial support)

JML: Alcon, Allergan, Bausch & Lomb, Carl Zeiss Meditec, Heidelberg Engineering, Reichert, Valeant Pharmaceuticals (Consultant); Bausch & Lomb, Carl Zeiss Meditec, Heidelberg Engineering, National Eye Institute, Optovue, Reichert, Topcon

CAG: National Eye Institute, EyeSight Foundation of Alabama, Research to Prevent Blindness, Carl Zeiss Meditec, Heidelberg Engineering, SOLX (financial support)

RMF, HD, YH, BCS, JFP, LAA-A, SCP, CT, JC, RB, PAS, GAC, DB, RR, NPB, LSB, GD: none FAM: Alcon, Allergan, Bausch + Lomb, Carl Zeiss Meditec, Heidelberg Engineering, Merck, Reichert, Sensimed and Topcon (financial support); Alcon, Allergan, Carl Zeiss Meditec, National Eye Institute, and Reichert (research support); Allergan, Carl Zeiss Meditec, Novartis (consultant)

SKD, JD, CDL, NDP, BIF, DWB, MCYN, YDIC, RA, JIR: none

RNW: Aerie Pharma, Allergan, Eyeovia, Unity Bio (Consultant); Bausch & Lomb, Centervue, Heidelberg Engineering, Carl Zeiss Meditec, Genentech, Optovue, Topcon (Financial support)

<sup>6</sup>Eye Care Center Management, Inc., Marrow, Georgia.

<sup>7</sup>Center for Genomics and Personalized Medicine Research, Wake Forest School of Medicine, Winston-Salem, North Carolina.

<sup>8</sup>Center for Public Health Genomics, Wake Forest School of Medicine, Winston-Salem, North Carolina.

<sup>9</sup>Department of Internal Medicine, Wake Forest School of Medicine, Winston-Salem, North Carolina.

<sup>10</sup>Department of Biochemistry, Wake Forest School of Medicine, Winston-Salem, North Carolina.

<sup>11</sup>Center for Diabetes Research, Wake Forest School of Medicine, Winston-Salem, North Carolina.

<sup>12</sup>Department of Biostatistical Sciences, Wake Forest School of Medicine, Winston-Salem, North Carolina.

<sup>13</sup>Einhorn Clinical Research Center, New York Eye and Ear Infirmary of Mount Sinai, New York, New York.

# These authors contributed equally to this work.

## Abstract

**Objective:** Find genetic contributions to glaucoma in African Americans.

**Design:** Cross-sectional, case-control study.

**Participants:** 1875 POAG cases and 1709 controls, self-identified as African Descent (AD), from the African Descent and Glaucoma Evaluation Study (ADAGESIII) and Wake Forest School of Medicine.

**Methods:** MegaChip genotypes were imputed to Thousand Genomes data. Association of SNPs with POAG and advanced POAG was tested by linear mixed model correcting for relatedness and population stratification. Genetic risk scores were tested by Receiver Operator Characteristics (ROC-AUC).

**Main Outcome:** POAG defined by visual field loss without other non-ocular conditions (N=1875). Advanced POAG was defined by age-based mean deviation of visual field (N=946).

**Results:** 18,281,920 SNPs met imputation quality  $r^2 > 0.7$  and minor allele frequency  $> 0.005$ . Association of a novel locus, *ENO4*, was observed for advanced POAG (rs185815146 beta 0.36, SE 0.065,  $p < 3 \times 10^{-8}$ ). For POAG, an AD signal was observed at *9p21* ED POAG signal (rs79721419;  $p < 6.5 \times 10^{-5}$ ) independent of the previously observed *9p21* ED signal (rs2383204;  $p < 2.3 \times 10^{-5}$ ) by conditional analyses. An association with POAG in *FNDC3B* (rs111698934,  $p < 3.9 \times 10^{-5}$ ) was observed, not in LD with the previously reported ED SNP. Additional previously identified loci associated with POAG in AD were: *8q22*, *AFAPI*, *TMCO1*. An AUC of 0.62 was observed with an unweighted genetic risk score composed of 11 SNPs in candidate genes. Two additional risk scores were studied by using a penalized matrix decomposition with cross-validation; risk scores of 50 and 400 SNPs were identified with ROC of AUC=0.74 and AUC=0.94, respectively.

**Conclusions:** A novel association with advanced POAG in the *ENO4* locus was putatively identified in subjects of African descent. In addition to this finding, this GWAS in AD POAG subjects contributes to POAG genetics by identification of novel signals in prior loci (*9p21*), as well as advancing the fine-mapping of regions due to shorter average linkage disequilibrium (*FNDC3B*). While not useful without confirmation and clinical trials, the use of genetic risk scores demonstrated that considerable AD-specific genetic information remains in these data.

## Precis

Genome-wide association study of POAG in subjects of African descent shows both similarities and differences with loci previously identified in large-scale studies of POAG in subjects of European Descent.

## INTRODUCTION

The African Descent and Glaucoma Evaluation Study (ADAGES) was designed to advance understanding of the greater susceptibility and higher rates of blindness due to primary open angle glaucoma (POAG) in individuals of sub-Saharan African continental descent (AD) such as US African Americans.<sup>1-3</sup> AD POAG patients tend to have worse visual field (VF) damage and progression of disease. For example, among glaucoma patients with elevated intra-ocular pressure (IOP), AD POAG patients were 5.2 times more likely to develop VF loss than individuals of European continental descent (ED).<sup>4</sup> Such examples of racial differences point to a genetic contribution to the pathophysiology of POAG.

This genetic component to POAG is consistent with accumulating evidence.<sup>5</sup> Rare forms of POAG affecting children and young adults are usually inherited as Mendelian disorders with either recessive or dominant inheritance of a single gene.<sup>5</sup> Linkage studies of POAG families have identified a role for the myocilin gene (*MYOC*; dbGENE 4653; OMIM 601652) in POAG.<sup>6, 7</sup> In contrast, common forms of POAG affecting adults over the age of 50 are inherited as non-Mendelian or complex traits. Several genome-wide association studies (GWAS) and meta-analyses for POAG have now been completed, mostly in ED populations. A strong and consistent finding across multiple ethnic groups is the association of POAG with the region including the cyclin dependent kinase inhibitor 2B region (*CDKN2B*; dbGENE 1030) and its antisense RNA *CDKN2B-AS* (dbGENE 100048912) at the *9p21* locus.<sup>8</sup> This association has been observed, for example, in Australian,<sup>9</sup> European,<sup>10</sup> Chinese,<sup>11</sup> Japanese,<sup>12, 13</sup> other Pacific Rim countries,<sup>10</sup> US Caucasian,<sup>14, 15</sup> Barbados,<sup>16</sup> and African-American<sup>17</sup> populations. This region was also among the first observed associations with coronary artery disease and type 2 diabetes,<sup>18, 19</sup> and accumulating evidence points to disruption of tissue-specific TGF-beta regulation in aortic smooth muscle cells.<sup>20, 21</sup> Additional POAG genes reaching genome-wide significance include: *AFAPI* (dbGENE 60312), *ATXN2* (dbGENE 6311),<sup>22</sup> *CAVI/CAV2* (dbGENE 857, 858),<sup>23</sup> *FOXCI/GMDS* (dbGENE 2296,2762),<sup>22, 24</sup> *SIX6* (dbGENE 4990),<sup>25</sup> *TGFBR3* (dbGENE 7048),<sup>10</sup> *TMCO1* (dbGENE 54499),<sup>9</sup> and *TXNRD2* (dbGENE 10587).<sup>22</sup> Recently, SNP rs76481776 in the microRNA (miRNA) gene *MIR182* (dbGENE 406958) has associated with POAG by the NEI Glaucoma Human Genetic Collaboration Heritable Overall Operational Database (NEIGHBORHOOD) consortium.<sup>26</sup> Functional analyses suggested that *MIR182* was

expressed in trabecular meshwork cells and was higher in the aqueous humor from glaucoma patients when compared with controls.

In this paper we present a GWAS of AD glaucoma patients from the ADAGESIII Contribution of Genotype to Glaucoma Phenotype in African Americans cohort.<sup>27</sup> We then compare our results with loci previously identified in both early onset and in adult glaucoma cases in ED populations.

## METHODS

### Subjects

The African Descent and Glaucoma Evaluation Study (ADAGESIII) has been described in our earlier publication.<sup>27</sup> “African Descent” and “AD” in this paper are defined as “Descent from sub-Saharan Africa.” Subjects in this report consist of POAG cases (n=2014) and controls (n=234) ascertained by the eye clinics of this consortium and additional “convenience controls” (n=2049) ascertained at Wake Forest School of Medicine. All subjects were self-identified for African Descent (AD). Advanced POAG was defined by age-based mean deviation:  $-10\text{dB}$  and age  $> 60$  yr, or  $-8\text{dB}$  and age  $>50$  yr, or  $-6\text{dB}$  and age  $> 40$  yr (n=946). This study was approved by the institution review boards of the clinical sites, the University of California San Diego, Wake Forest School of Medicine, and Los Angeles Biomedical Research Institute.

### Generation of Genomic Data

**Genotyping.**—DNA was isolated from either whole blood or saliva from subjects ascertained by ADAGES and at Wake Forest School of Medicine (WFSM). These samples were genotyped using the Illumina MegaChip (Illumina, San Diego, CA) in the LA Biomed Genomics Center and the Center for Genomics and Personalized Medicine Research at WFSM, respectively. Output files (“idat files”) from both LA Biomed and WFSM were merged and genotypes were called across both studies as a single project using the Illumina software (GenomeStudio 2.0).<sup>28, 29</sup> This “common calling” provided genotype data for 2049 WFSM controls, 2014 ADAGES POAG cases, and 234 ADAGES controls. Subjects were removed for failed genotyping, unresolvable gender discrepancies, being outliers by principal component analyses, and by relatedness with  $\hat{\pi} > 0.2$ . Genotyping rates were  $>99\%$  per subject and  $> 99\%$  per single nucleotide polymorphism (SNP). The final dataset consisted of 870,067 autosomal SNPs with a minor allele frequency (MAF)  $>0.005$  in 1875 POAG cases and 1709 controls.

**AD Estimate.**—Genotype data for Chromosomes 1-22 were pruned for linkage disequilibrium (PLINK, at  $r^2 < 0.2$ ) and the amount of AD for each subject was estimated by an unsupervised analysis using Admixture 1.3.0 with  $K=3$  for sub-Saharan African, European, and Native American continental ancestries.<sup>30, 31</sup> “K,” or the number of populations expected in the analysis, was set at 3 because ADAGESIII recruits AD POAG cases from San Diego, New York, Alabama, Georgia, and Texas, and while research subjects self-identify as AD, they may also have an additional and different Native American contributions.

**Imputation.**—SNP data were uploaded to the Michigan Imputation Server for imputation to the 1kGP phase 3 dataset.<sup>32</sup> SNP data with imputation quality score > 0.70 and minor allele frequency (MAF) > 0.005 were then tested for discrepancies between allele frequencies in the ADAGES and WFSM controls and removed if a Hardy-Weinberg test was significant (p-value < 0.05). A total of 18,281,920 autosomal SNPs were tested for association.

## Genetic Analyses

**Association with POAG and advanced POAG.**—The association of a SNP with POAG or advanced POAG was tested using a fast, variance components, mixed model approach (EMMAX).<sup>33, 34</sup> The use of a mixed model association test with correction by a genetic relationship matrix provided superior correction for population stratification and genetic relatedness.<sup>35, 36</sup> Covariates were Principal Components 1-3. Subjects over 8 standard deviations from the center of each component were removed (smartPCA). Since the glaucoma patients are recruited at tertiary referral centers, we did not observe an association with age and sex with these two phenotypes and so these were not included as covariates.

**Candidate Gene Study.**—Both rare and common previously identified genetic variants were selected as candidate genes for study;<sup>5, 37, 38</sup> the list included variants contributing to early onset POAG and factors with genome-wide significance for POAG identified by GWAS. We tested 35,865 SNPs for association in this part of the study; these SNPs are located between the start and end of transcription in the following 25 loci: *8q22*<sup>14</sup>, *9p21*<sup>7, 8, 14</sup>, *ABCA1*<sup>11, 24</sup>, *ABO*<sup>39</sup>, *AFAP1*<sup>40</sup>, *ARHGEF12*<sup>41</sup>, *ATOH7*<sup>42</sup>, *ATXN2*<sup>6, 22</sup>, *CAV1*<sup>23, 43</sup>, *CYP1B1* (OMIM#231300), *FNDC3B*<sup>10</sup>, *GAS7*<sup>22</sup>, *FOXC1/GMDS*<sup>15, 22</sup>, *LTBP2* (OMIM#613086)<sup>13</sup>, *MIR182*<sup>26</sup>, *MYOC* (OMIM\*601652)<sup>7</sup>, *OPTN* (OMIM#137760), *PMM2*<sup>11</sup>, *SIX1/SIX2*<sup>25</sup>, *TBK1* (OMIM#177700), *TGFBR3*<sup>10</sup>, *TMOCP*<sup>9</sup>, and *TXNRD2*<sup>22</sup>. Association with POAG and advanced POAG was tested as above. The list of loci and SNPs tested is in Supplemental Table 1.

**Rationale for Genetic Risk Scores.**—In addition to being composed of highly significant GWAS SNPs only, genetic risk scores may also be composed of moderately significant GWAS SNPs since it is well-known that: (1) GWAS results contain a mix of “true positive” and “false positive” loci, and (2) “true positive” loci will contribute to the ability of the score to discriminate phenotype or disease and “false positive” loci will contribute “noise”.<sup>44-46</sup> We tested two types of score: for Genetic Risk Score #1, SNPs were selected from the well-identified loci associated in this study (11 SNPs, see Table 2); for Genetic Risk Score #2 SNPs were selected from all SNPs showing some association with AD POAG (~12,900 SNPs with an association p-value less than 0.001). Since all ~12,900 SNPs together did not produce a usable genetic risk score (see below), in order to enrich for “true positives” over “false positives,” or “signal” over “noise,” a regularized (also known as a penalized) method was applied. Furthermore, regularized methods work well when the number of SNPs is much greater than the number of subjects, as in this study and are robust to correlation between SNPs.<sup>47</sup> The following should be noted: first, this analysis is *not* the same as using SNPs with the highest effect sizes in the model because the use of regularization tests the SNPs together, not individually; and second, the original

development of receiver operating characteristics was in the context of “signal” over “noise” and so is appropriate for this context for selecting “true positives” from “false positives.”

**Genetic Risk Score #1.**—We selected SNPs for this score (a) associated with POAG or advanced POAG from ED and AD SNPs with p-value < 0.001, imputation  $r^2 < 0.7$ ,  $maf > 0.005$ , and one per locus (Table 2) were used to calculate genetic risk score #1 for POAG. First, the genotypes of SNPs with negative effect sizes were re-coded to the other allele so that the number of “risk” alleles for each SNP was additive for increased POAG risk, *i.e.* an “unweighted score.” Table 2 shows how these 11 SNPs perform together in a single logistic regression model. These allele counts were then added for each subject in order to provide the genetic risk score. The utility of this score for prediction of POAG within this dataset was then tested by estimating the area under the receiver-operator characteristic (AUC; ROC).<sup>48</sup> The R package “ROCR” was used for calculating ROC and plotting AUC.<sup>44</sup> (<http://rocr.bioinf.mpi-sb.mpg.de>)

**Genetic Risk Scores #2 and #3.**—All SNPs associated with POAG or advanced POAG with p-values < 0.001 were used to calculate Genetic Risk Score #2 and #3 for POAG. Genotypes of the SNPs in this subset with negative effect sizes (betas) were re-coded to the other allele so that the number of “risk” alleles for each SNP was additive for increased POAG risk. These allele counts were then added for each subject in order to provide the genetic risk score, *i.e.* “unweighted” risk score. Since the number of SNPs greatly exceeded the number of subjects, a penalized logistic regression was employed with 10-fold cross-validation to find the SNP subset associated with increased POAG risk (R package GLMNET).<sup>47, 49</sup> This approach combined a maximum likelihood method to test significance with coordinate descent to choose the penalty.<sup>50</sup> The greater the penalty, the fewer SNPs that remain in the model. This analysis was performed with two different penalties: one (Genetic Risk Score #2) that would provide 40-50 SNPs in the score, the second (Genetic Risk Score #3) that would provide 400-500 SNPs in the score. The utility of both Genetic Score #2 and #3 was then tested by receiver operating characteristics as for Genetic Risk Score #1.

## RESULTS

Inflation due to population stratification and cryptic relatedness was minimal for SNPs with minor allele frequencies (MAF) greater than 0.005 (Supplemental Figures 1 & 2;  $\lambda_s$  for POAG was 1.017 and for advanced POAG 1.022). The final genotype dataset consisted of ~18.3 million SNPs with imputation scores > 0.7 and MAF > 0.005 in controls. After quality control of sample data, there were 1875 AD POAG cases (of which 946 had advanced POAG) and 1709 AD “convenience” controls.

### Putative AD Novel Locus

An association of advanced POAG with the *ENO4* locus was observed at SNP rs185815146 (Fig. 1A, “Manhattan” plot; Fig. 1B, “LocusZoom” plot). The effect allele frequency (“A”) in cases was 0.029 and in controls 0.007, the effect size (beta) = 0.36 with standard error = 0.065, p-value =  $3.0 \times 10^{-8}$ . In Thousand Genomes Project data (1kGP), this SNP has only been observed in the African and African American populations (AD; dbSNP). The hg19

coordinates of this SNP are at Chr10:118,623,580 and the *ENO4* locus is located between the *HSPA12A* and *SHTNI* (aka *KIAA1598*) loci. No SNP was associated with POAG at the genome-wide significance level (Supplementary Fig. 3).

### Previously Identified Loci

The association results were further examined within the regions of loci previously reported to be associated with POAG (Table 1 and Supplementary Table 1).

**9p21/CDKN2B.**—The first observed pattern of association was that of an additional, independent AD signal in a previously identified locus for POAG. The most significant and consistent association with POAG observed in previous GWAS studies has been the *9p21* locus.<sup>8</sup> This *9p21* association was confirmed with AD POAG (rs2383204, *9p21* Signal #1; Table 1 and Fig. 2A). This SNP is in LD with the previously reported ED SNPs rs1063192<sup>42</sup> and rs4977756.<sup>9</sup> A second association signal at SNP rs79721419 was observed (*9p21* Signal #2; Table 1 and Fig. 2B). There was no LD between Signal #1, rs2383204, and Signal #2, rs79721419, and a region of high recombination rate in the 1kGP AFR subset separates them; this subset includes AD subjects from the Southwest US (ASW). The independence of these two association signals was tested by conditional analyses; the association at rs2383204 remained when conditioning on rs79721519 (Fig. 2C), and the association at rs79721419 remained when conditioning on rs2383204 (Fig. 2D). Since the rs2383204 signal has been observed in European populations, this independence supported the concept that the rs2383204 signal is of European continental origin and the rs79721419 was of African continental origin.

**FNDC3B with POAG; GAS7 with advanced POAG.**—Two loci showed the second pattern: (1) a SNP associated with either POAG or advanced POAG, (2) no LD with previously reported ED SNPs, and (3) separated from the previously reported ED SNP(s) by a region of high recombination rate in the 1kGP AFR subset. SNP rs199612704 in the *FNDC3B* locus was associated with POAG (Table 1); this SNP was not in LD with the previously reported ED SNPs rs12897 or rs4894796, and is separated by a region of high recombination (Fig. 3A and B). Similarly, SNP rs8080535 in the *GAS7* locus was associated with advanced POAG (Supplementary Table 1); this SNP is not in LD with the previously reported ED SNPs rs9897123, rs9913911, or rs121502840, and was separated by a region of high recombination (Fig. 3C&D).<sup>22, 39, 51</sup> These observations support the concept that SNPs contributing to POAG and advanced POAG are present in AD subjects, but additional to the SNPs reported for ED.

**8q22, AFAP1.**—A third pattern was observed: an associated SNP not in LD with previously reported SNPs or separated by a region of high recombination, “same locus different SNP.” SNP rs7009228 in the 8q22 locus was associated with POAG (Table 1) but was not in LD with the previously reported ED SNPs rs1521444, rs284489, or rs284495.<sup>14</sup> SNP rs4328916 in the *AFAP1* locus was associated with POAG but was not in LD with ED SNP rs4619890.<sup>24</sup>

**TMCO1.**—The fourth pattern observed was that of a SNP associated with POAG and *is* in LD with previously reported ED SNPs. SNP rs10529326 in the *TMCO1* locus is in LD with ED SNPs rs4656461 and rs7518099.<sup>9</sup> We observed an association with this last SNP and POAG.

### Genetic Risk Score for POAG

**Genetic Risk Score #1.** First, 11 loci associated with POAG were selected (Table 2) from ED and AD SNPs associated with POAG (Table 2). We included top SNPs with African-specific signals for this model. Genotypes were first recoded to the opposite strand if the effect estimate (beta) was negative and then allele counts were added. In this way, a higher score will be associated with greater risk for POAG. This produced an unweighted score that varied between 2 and 15 (Fig. 4A, 11 SNPs). Next, this score was then tested for its ability to predict POAG using receiver operation characteristics (ROC), and an area under the curve (AUC) value of 0.62 was observed (Fig. 4B, blue solid line). For comparison, the null result of AUC=0.5 is included in Fig.4 (Fig. 4B, dotted black line).

**Genetic Risk Score #2 & #3.**—First, genotypes for ~12,900 SNPs (all SNPs with p-value < 0.001) were recoded to the opposite strand if the effect estimate (beta) was negative. As above, this provides an unweighted, greater score value with greater POAG risk. Next, in order to improve “signal” over “noise”, a regularized 10-fold cross-validation procedure was applied to find a subset of the ~12,900 SNPs that *together* have the highest ability to predict POAG.<sup>50</sup> For Genetic Risk Score #2, the penalty was selected to result in 40-50 SNPs for the score, and for #3, the penalty was selected to result in 400-500 SNPs for the score (Fig. 4A for both scores). Then, the ability of these scores to predict POAG was tested further by calculating ROC; the AUC for Genetic Risk Score #2 was 0.74 (Fig. 4B, green solid line) and for #3 was 0.94 (Fig. 4B, red solid line). For comparison, the solid black line shows the AUC for all ~12,900 SNPs (equal to 0.55).

## DISCUSSION

The results of our GWAS of POAG and advanced POAG in AD subjects suggested that a novel locus, *ENO4*, is associated with advanced POAG in AD, that novel SNPs in the already identified loci, *9p21* and *FNDC3B* are associated with POAG, and that novel SNPs in the already identified locus *GAS7* are associated with advanced POAG.

### Novel Loci

***ENO4* & advanced POAG.**—A putative novel finding was the association of advanced POAG with the enolase 4 gene (*ENO4*; dbGENE 387712; Fig. 1); this locus is located on Chromosome 10 at position 118,623,580 (SNP rs185815146; “A” allele; genome build hg19). SNP rs185815146 has been observed only in the AFR sub-set of the 1kGP data. This finding should be considered preliminary pending further collaborations to enlarge the sample size and to confirm results across African Descent datasets. One of the weaknesses of our study is that we do not have a confirmation dataset to confirm this finding at this time. However, we propose this locus for POAG of subjects with African Descent because (a) the minor allele is found only in African populations, (b) Expression of *ENO4* and the flanking



genes *HSPA12A* and *SHTNI* has been observed in POAG-related tissues, *e.g.* the optic nerve head and the trabecular meshwork (Ocular Tissue Database; <https://genome.uiowa.edu/otdb>),<sup>53</sup> (c) using the advanced POAG sample size, our study has 0.69 power to detect an effect size of 2.5 at MAF 0.005, at genomewide significance, assuming there are 100 loci associated with POAG and greater than 0.8 at effect size 2.2 and MAF 0.01 for the 100 loci model and at effect size 2.4 and MAF 0.015 for a 25 locus model. The role of metabolism in the pathophysiology of POAG is suggested by the fact that the enolase 4 enzyme (4.2.1.11) participates in glucose metabolism as a proximal step to phosphoenol pyruvate (KEGG).

### Utility of Studying Multiple Ethnic Groups

Our findings reinforce the rationale for performing GWAS in multiple US populations (summarized in Table 3): (a) potential to find new genes, (b) find population-specific associations that may shed additional light on the role of that locus in disease development, (c) find recombination events that may allow finer mapping of an association due to the shorter linkage disequilibrium in populations of African descent, and (d) provide a “natural mix” of disease loci from both European descent and African descent genomic segments to allow study of the related genes in different combinations.

### Genetic Risk Score

For Genetic Risk Score #1, the sum of the allele counts across the 11 SNPs from the candidate gene study (Tables 1 and 2) resulted in a genetic risk score with an area under the curve (AUC) value of 0.62 (Fig. 4). For Genetic Risk Scores #2 & #3, allele counts across the all of the ~12,900 SNPs with p-values less than 0.001 resulted in a score with an AUC of 0.55 (Fig. 4B, solid black line). The fact that this score is lower than the AUC for score #1 for suggests that noise is being introduced from SNPs in the ~12,900 that do not contribute to the determination of POAG risk. Thus, in order to find the combination of SNPs within the 12,900 that *together* are associated with greater POAG risk, a regularized matrix decomposition method was applied. Regularization methods are recommended for the type of “big data” problem represented here where the number of features (~12,900 SNPs) is much greater than the number of subjects (1875 POAG cases and 1709 controls).<sup>49</sup> The penalty was selected to result in 40-50 SNPs (Genetic Risk Score #2) and 400-500 SNPs (Genetic Risk Score #3) contributing to the risk score. 10-fold cross-validation at each penalty value is used to test the ability to predict POAG. The AUC value for Genetic Risk Score #2 was 0.74 and for #3 was 0.94. We emphasize for this report: *the requisite confirmation studies and prospective clinical trials required to design a valid genetic test for AD POAG risk have not been completed and so this genetic risk score is not suitable for clinical prediction at this time.* However, the AUC *difference* between the AUC values of Genetic Risk Score #1 and Genetic Risk Score #2 and #3 clearly indicates that there are additional SNPs that contribute to AD POAG risk even though these did not meet the multiple testing criteria required for either a candidate gene study or a genome-wide study. The identification of additional loci will be possible as meta-analyses are conducted by worldwide collaborations and their overall contribution to POAG risk will be elucidated by the methods used here.

In conclusion, this candidate gene study of POAG and advanced POAG in AD subjects has fulfilled some of its promise for the genetic study of POAG, revealing additional SNPs in already identified loci, narrowing of regions by the different linkage disequilibrium structure of AD possible, and supporting the concept that further loci are waiting to be revealed.

## Supplementary Material

Refer to Web version on PubMed Central for supplementary material.

## Acknowledgments

Financial Support

National Eye Institute: EY023704, P30EY022589, EY110008, EY019869, EY021818 National Institutes of Health: R01 DK087914, R01 DK066358, R01 DK053591, U01 DK105556, R01 HL56266, R01 DK070941, DRC DK063491, and CTSI UL1TR001881

## References

1. Sample PA, Girkin CA, Zangwill LM, et al. The African Descent and Glaucoma Evaluation Study (ADAGES): design and baseline data. *Arch Ophthalmol* 2009;127(9): 1136–45. [PubMed: 19752422]
2. Girkin CA, Sample PA, Liebmann JM, et al. African Descent and Glaucoma Evaluation Study (ADAGES): II. Ancestry differences in optic disc, retinal nerve fiber layer, and macular structure in healthy subjects. *Arch Ophthalmol* 2010;128(5):541–50. [PubMed: 20457974]
3. Racette L, Liebmann JM, Girkin CA, et al. African Descent and Glaucoma Evaluation Study (ADAGES): III. Ancestry differences in visual function in healthy eyes. *Arch Ophthalmol* 2010;128(5):551–9. [PubMed: 20457975]
4. Khachatryan N, Medeiros FA, Sharpsten L, et al. The African Descent and Glaucoma Evaluation Study (ADAGES): predictors of visual field damage in glaucoma suspects. *Am J Ophthalmol* 2015;159(4):777–87. [PubMed: 25597839]
5. Wang R, Wiggs JL. Common and rare genetic risk factors for glaucoma. *Cold Spring Harb Perspect Med* 2014;4(12):a017244. [PubMed: 25237143]
6. Allingham RR, Wiggs JL, De La Paz MA, et al. Gln368STOP myocilin mutation in families with late-onset primary open-angle glaucoma. *Invest Ophthalmol Vis Sci* 1998;39(12):2288–95. [PubMed: 9804137]
7. Wiggs JL, Allingham RR, Vollrath D, et al. Prevalence of mutations in TIGR/Myocilin in patients with adult and juvenile primary open-angle glaucoma. *Am J Hum Genet* 1998;63(5): 1549–52. [PubMed: 9792882]
8. Ng SK, Casson RJ, Burdon KP, Craig JE. Chromosome 9p21 primary open-angle glaucoma susceptibility locus: a review. *Clin Exp Ophthalmol* 2014;42(1):25–32. [PubMed: 24112133]
9. Burdon KP, Macgregor S, Hewitt AW, et al. Genome-wide association study identifies susceptibility loci for open angle glaucoma at TMCO1 and CDKN2B-AS1. *Nat Genet* 2011;43(6):574–8. [PubMed: 21532571]
10. Li Z, Allingham RR, Nakano M, et al. A common variant near TGFBR3 is associated with primary open angle glaucoma. *Hum Mol Genet* 2015;24(13):3880–92. [PubMed: 25861811]
11. Chen Y, Lin Y, Vithana EN, et al. Common variants near ABCA1 and in PMM2 are associated with primary open-angle glaucoma. *Nat Genet* 2014;46(10): 1115–9. [PubMed: 25173107]
12. Takamoto M, Kaburaki T, Mabuchi A, et al. Common variants on chromosome 9p21 are associated with normal tension glaucoma. *PLoS One* 2012;7(7):e40107. [PubMed: 22792221]
13. Osman W, Low SK, Takahashi A, et al. A genome-wide association study in the Japanese population confirms 9p21 and 14q23 as susceptibility loci for primary open angle glaucoma. *Hum Mol Genet* 2012;21(12):2836–42. [PubMed: 22419738]

14. Wiggs JL, Yaspan BL, Hauser MA, et al. Common variants at 9p21 and 8q22 are associated with increased susceptibility to optic nerve degeneration in glaucoma. *PLoS Genet* 2012;8(4):e1002654. [PubMed: 22570617]
15. Pasquale LR, Loomis SJ, Kang JH, et al. CDKN2B-AS1 genotype-glaucoma feature correlations in primary open-angle glaucoma patients from the United States. *Am J Ophthalmol* 2013;155(2):342–53 e5. [PubMed: 23111177]
16. Cao D, Jiao X, Liu X, et al. CDKN2B polymorphism is associated with primary open-angle glaucoma (POAG) in the Afro-Caribbean population of Barbados, West Indies. *PLoS One* 2012;7(6):e39278. [PubMed: 22761751]
17. Liu Y, Hauser MA, Akafo SK, et al. Investigation of known genetic risk factors for primary open angle glaucoma in two populations of African ancestry. *Invest Ophthalmol Vis Sci* 2013;54(9):6248–54. [PubMed: 23963167]
18. Diabetes Genetics Initiative of Broad Institute of H, Mit LU, Novartis Institutes of BioMedical R, et al. Genome-wide association analysis identifies loci for type 2 diabetes and triglyceride levels. *Science* 2007;316(5829):1331–6. [PubMed: 17463246]
19. Samani NJ, Erdmann J, Hall AS, et al. Genomewide association analysis of coronary artery disease. *N Engl J Med* 2007;357(5):443–53. [PubMed: 17634449]
20. Chen HH, Almontashiri NA, Antoine D, Stewart AF. Functional genomics of the 9p21.3 locus for atherosclerosis: clarity or confusion? *Curr Cardiol Rep* 2014;16(7):502. [PubMed: 24893939]
21. Almontashiri NA, Antoine D, Zhou X, et al. 9p21.3 Coronary Artery Disease Risk Variants Disrupt TEAD Transcription Factor-Dependent Transforming Growth Factor beta Regulation of p16 Expression in Human Aortic Smooth Muscle Cells. *Circulation* 2015;132(21):1969–78. [PubMed: 26487755]
22. Bailey JN, Loomis SJ, Kang JH, et al. Genome-wide association analysis identifies TXNRD2, ATXN2 and FOXC1 as susceptibility loci for primary open-angle glaucoma. *Nat Genet* 2016;48(2):189–94. [PubMed: 26752265]
23. Loomis SJ, Kang JH, Weinreb RN, et al. Association of CAV1/CAV2 genomic variants with primary open-angle glaucoma overall and by gender and pattern of visual field loss. *Ophthalmology* 2014;121(2):508–16. [PubMed: 24572674]
24. Gharahkhani P, Burdon KP, Fogarty R, et al. Common variants near ABCA1, AFAP1 and GMDS confer risk of primary open-angle glaucoma. *Nat Genet* 2014;46(10):1120–5. [PubMed: 25173105]
25. Carnes MU, Liu YP, Allingham RR, et al. Discovery and functional annotation of SIX6 variants in primary open-angle glaucoma. *PLoS Genet* 2014;10(5):e1004372. [PubMed: 24875647]
26. Liu Y, Bailey JC, Helwa I, et al. A Common Variant in MIR182 Is Associated With Primary Open-Angle Glaucoma in the NEIGHBORHOOD Consortium. *Invest Ophthalmol Vis Sci* 2016;57(10):3974–81. [PubMed: 27479813]
27. Zangwill LM, Ayyagari R, Liebmann JM, et al. The African Descent and Glaucoma Evaluation Study (ADAGES) III: Contribution of genotype to glaucoma phenotype in African-Americans: Study design and baseline data *Ophthalmology* 2018;in press.
28. Gunderson KL, Steemers FJ, Lee G, et al. A genome-wide scalable SNP genotyping assay using microarray technology. *Nat Genet* 2005;37(5):549–54. [PubMed: 15838508]
29. Gunderson KL, Kuhn KM, Steemers FJ, et al. Whole-genome genotyping of haplotype tag single nucleotide polymorphisms. *Pharmacogenomics* 2006;7(4):641–8. [PubMed: 16768648]
30. Alexander DH, Novembre J, Lange K. Fast model-based estimation of ancestry in unrelated individuals. *Genome Res* 2009;19(9):1655–64. [PubMed: 19648217]
31. Alexander DH, Lange K. Enhancements to the ADMIXTURE algorithm for individual ancestry estimation. *BMC Bioinformatics* 2011;12:246. [PubMed: 21682921]
32. Das S, Forer L, Schonherr S, et al. Next-generation genotype imputation service and methods. *Nat Genet* 2016;48(10):1284–7. [PubMed: 27571263]
33. Kang HM, Sul JH, Service SK, et al. Variance component model to account for sample structure in genome-wide association studies. *Nat Genet* 2010;42(4):348–54. [PubMed: 20208533]
34. Price AL, Zaitlen NA, Reich D, Patterson N. New approaches to population stratification in genome-wide association studies. *Nat Rev Genet* 2010;11(7):459–63. [PubMed: 20548291]

35. Conomos MP, Laurie CA, Stilp AM, et al. Genetic Diversity and Association Studies in US Hispanic/Latino Populations: Applications in the Hispanic Community Health Study/Study of Latinos. *Am J Hum Genet* 2016;98(1):165–84. [PubMed: 26748518]
36. Chen H, Wang C, Conomos MP, et al. Control for Population Structure and Relatedness for Binary Traits in Genetic Association Studies via Logistic Mixed Models. *Am J Hum Genet* 2016;98(4): 653–66. [PubMed: 27018471]
37. Wiggs JL, Pasquale LR. Genetics of glaucoma. *Hum Mol Genet* 2017;26(R1):R21–R7. [PubMed: 28505344]
38. Lewis CJ, Hedberg-Buenz A, DeLuca AP, et al. Primary congenital and developmental glaucomas. *Hum Mol Genet* 2017;26(R1):R28–R36. [PubMed: 28549150]
39. Hysi PG, Cheng CY, Springelkamp H, et al. Genome-wide analysis of multi-ancestry cohorts identifies new loci influencing intraocular pressure and susceptibility to glaucoma. *Nat Genet* 2014;46(10):1126–30. [PubMed: 25173106]
40. Cook JP, Morris AP. Multi-ethnic genome-wide association study identifies novel locus for type 2 diabetes susceptibility. *Eur J Hum Genet* 2016;24(8): 1175–80. [PubMed: 27189021]
41. Springelkamp H, Iglesias AI, Cuellar-Partida G, et al. ARHGEF12 influences the risk of glaucoma by increasing intraocular pressure. *Hum Mol Genet* 2015;24(9):2689–99. [PubMed: 25637523]
42. Ramdas WD, van Koolwijk LM, Lemij HG, et al. Common genetic variants associated with open-angle glaucoma. *Hum Mol Genet* 2011;20(12):2464–71. [PubMed: 21427129]
43. Thorleifsson G, Walters GB, Hewitt AW, et al. Common variants near CAV1 and CAV2 are associated with primary open-angle glaucoma. *Nat Genet* 2010;42(10):906–9. [PubMed: 20835238]
44. Haritunians T, Taylor KD, Targan SR, et al. Genetic predictors of medically refractory ulcerative colitis. *Inflamm Bowel Dis* 2010;16(11):1830–40. [PubMed: 20848476]
45. Lubitz SA, Yin X, Lin HJ, et al. Genetic Risk Prediction of Atrial Fibrillation. *Circulation* 2017;135(14):1311–20. [PubMed: 27793994]
46. Cooke Bailey JN, Igo RP. Genetic Risk Scores. *Current Protocols in Human Genetics* 2016;91(9): 1.29.1–1.9.
47. Lange K, Papp JC, Sinsheimer JS, Sobel EM. Next Generation Statistical Genetics: Modeling, Penalization, and Optimization in High-Dimensional Data. *Annu Rev Stat Appl* 2014;1(1):279–300. [PubMed: 24955378]
48. Power Dudbridge F. and predictive accuracy of polygenic risk scores. *PLoS Genet* 2013;9(3):e1003348. [PubMed: 23555274]
49. Hastie T, Tibshirani R, Friedman JH. *The elements of statistical learning : data mining, inference, and prediction*, 2nd ed. New York, NY: Springer, 2009; xxii, 745 p.
50. Friedman J, Hastie T, Tibshirani R. Regularization Paths for Generalized Linear Models via Coordinate Descent. *J Stat Softw* 2010;33(1): 1–22. [PubMed: 20808728]
51. Verma SS, Cooke Bailey JN, Lucas A, et al. Epistatic Gene-Based Interaction Analyses for Glaucoma in eMERGE and NEIGHBOR Consortium. *PLoS Genet* 2016;12(9):e1006186. [PubMed: 27623284]
52. Nag A, Lu H, Arno M, et al. Evaluation of the Myocilin Mutation Gln368Stop Demonstrates Reduced Penetrance for Glaucoma in European Populations. *Ophthalmology* 2017;124(4):547–53. [PubMed: 28038983]
53. Wagner AH, Anand VN, Wang WH, et al. Exon-level expression profiling of ocular tissues. *Exp Eye Res* 2013;111:105–11. [PubMed: 23500522]
54. van Koolwijk LM, Ramdas WD, Ikram MK, et al. Common genetic determinants of intraocular pressure and primary open-angle glaucoma. *PLoS Genet* 2012;8(5):e1002611. [PubMed: 22570627]
55. Turner SD. qqman: An R package for visualizing GWAS results using Q-Q and manhattan plots. *bioRxiv*, 2014.
56. Pruim RJ, Welch RP, Sanna S, et al. LocusZoom: regional visualization of genome-wide association scan results. *Bioinformatics* 2010;26(18):2336–7. [PubMed: 20634204]

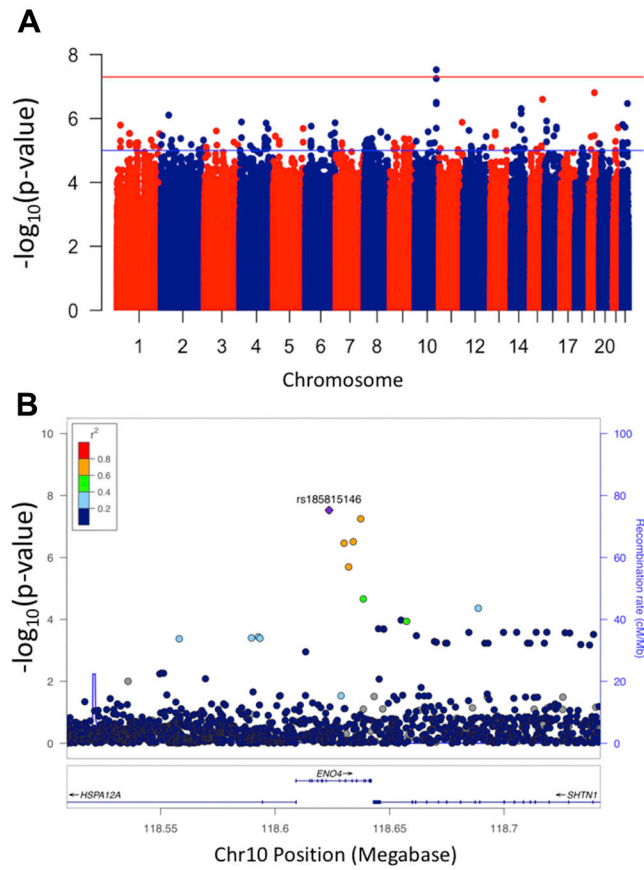


**Figure 1. Genome-wide association with advanced POAG.**

A) Manhattan plot showing association with advanced POAG in AD subjects. Plot generated using R package “qqman”.<sup>55</sup> Red line indicates p-value of  $5 \times 10^{-8}$ ; point above red line is rs185815146. B) LocusZoom plot of *ENO4* locus. Plot generated using the LocusZoom “standalone” program. Color of points shows linkage disequilibrium (LD) between rs185815146 and the other SNPs as found in the 1kGP data subset of sub-Saharan Africans (AFR). No LD between rs185815146 and the other SNPs was observed using the “EUR” subset.

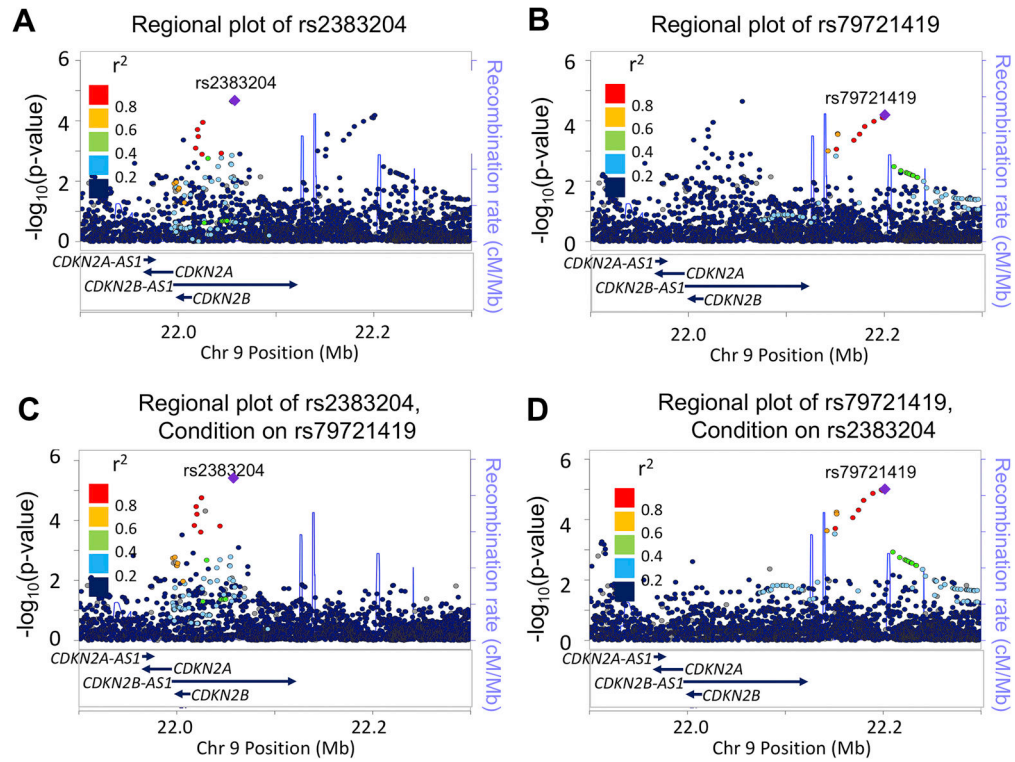


**Figure 2. The 9p21 Locus and AD POAG**

Association results from the ~5300 SNPs between 21.9 Megabases (Mb) and 22.4 Mb on Chromosome 9. Linkage disequilibrium values (LD; colors) are from the AFR subset of the 1kGP data; this subset includes African-Americans from the Southwestern U.S. (ASW) and were calculated using the LocusZoom “Standalone” program.<sup>56</sup> Blue lines indicate the recombination rate in centimorgans/million basepairs (cM/Mb) in the AMR data subset. (A) Association results with POAG; colors represent LD with rs2383204. (B) The same association results with POAG; colors represent LD with rs79721419. (C) Association with POAG conditioned on rs79721419; colors represent LD with rs2383204. Two previously reported SNPs were also in LD with rs2383204 and associated with POAG: rs1063192 (estimate, 0.052,  $p=0.013$ ) and rs518394 (estimate  $-0.056$ ,  $p=0.0063$ ). (D) Association with POAG, conditioned on rs2383204; colors represent LD with rs79721419. The same two previously reported SNPs, rs1063192 and rs518394 were not significant. In addition, no statistical interaction was observed between rs2383204 and rs79721419 in a general linear model with POAG as the outcome variable (Table 2).

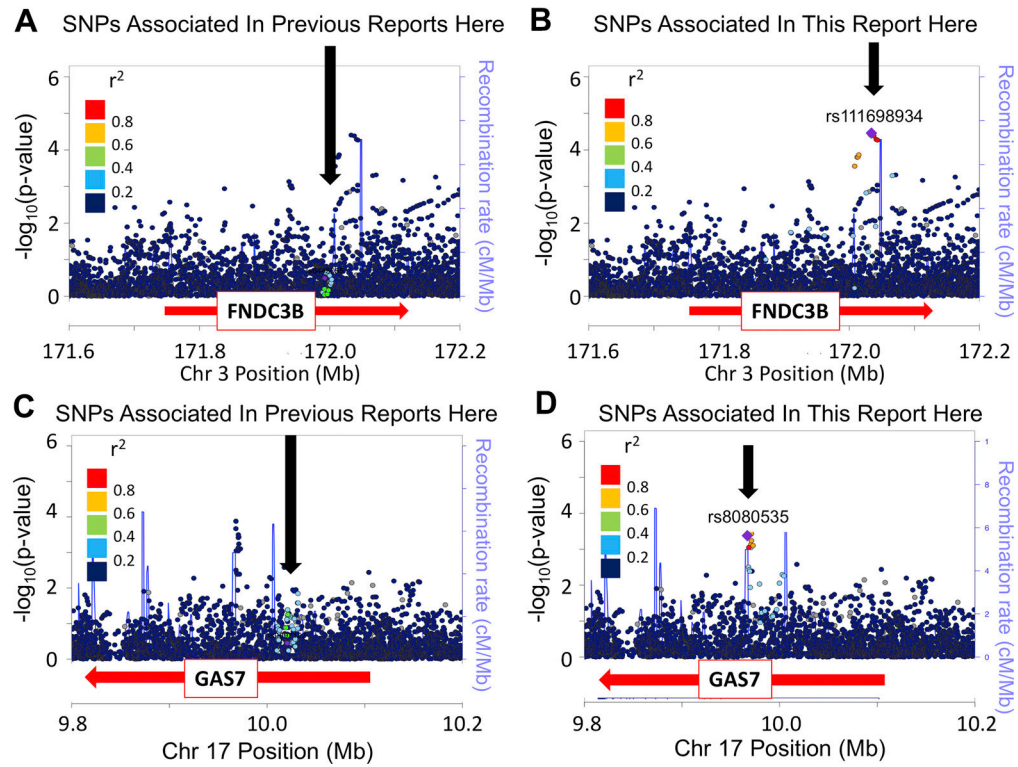


**Figure 3. Two Similar Results: Association of *FNDC3B* with POAG and *GAS7* with Advanced POAG**

LocusZoom Plots produced using the LocusZoom “Standalone” version. AFR LD values are in color. Blue lines indicate the recombination rate in AFR (cM/Mb). (A) *FNDC3B* gene and POAG. LD with rs12897, previously reported to be associated with POAG but not associated here in African-Americans. (B) *FNDC3B* gene and POAG. The same association results with the colors representing LD, with rs11698934. (C) *GAS7* gene and severity. LD with rs9913911, previously reported to be associated with POAG but not associated here in African-Americans. (D) *GAS7* gene and severity. The same association results with the colors representing LD, with rs8080535.

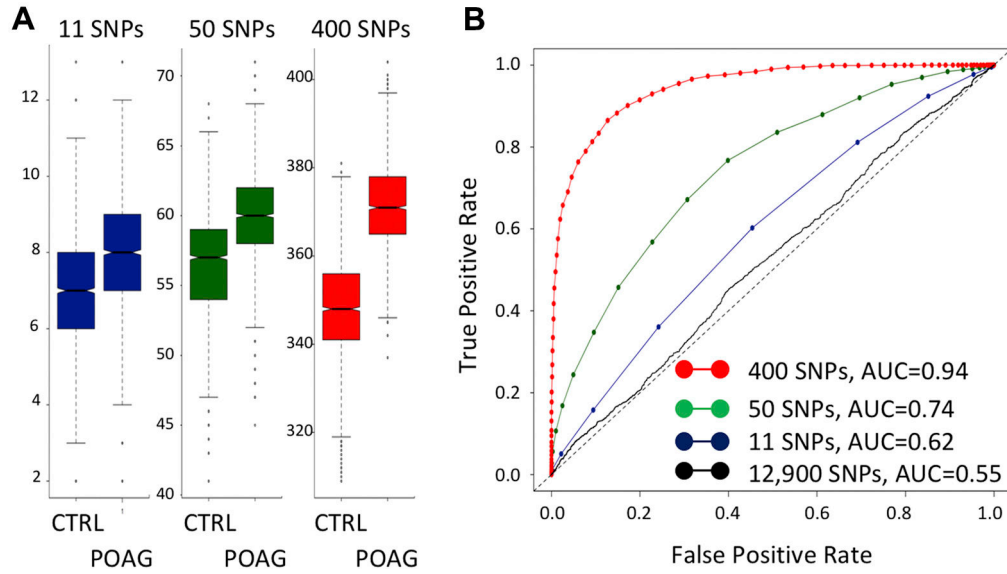


**Figure 4. Test of Genetic Risk Scores by Receiver Operating Characteristics**

Genetic risk scores were created by adding allele counts across selected SNPs for each subject; a SNP with a negative estimate (beta) was recoded to the other allele so that genotype counts would be additive for POAG risk. SNPs for Genetic Risk Score #1 were the 11 significantly associated SNPs in Table 1 (B, blue line). SNPs for Genetic Risk Score #2 were 50 SNPs selected using a penalized logistic regression and cross-validation procedure (B, green line). SNPs for Genetic Risk Score #3 were 400 SNPs selected by the same penalized logistic regression and cross-validation procedure (B, red line). For comparison, AUC=0.5 is the dotted black line, and AUC from all ~12,900 SNPs is the solid black line. CTRL, controls; POAG, cases.



**Table 1.**

Candidate Genes Associated with POAG and with Advanced POAG in AD Subjects

Phenotype	Locus	SNP	Chr	Position (hg19)	“Other” Allele	Effect Allele	Effect Size	Standard Error	P value	Reference Example
POAG	<i>TGFBR3</i>	rs11466588	1	92,293,416	C	A	0.190	0.056	6.5×10 <sup>-4</sup>	10
POAG	<i>TMCO1</i>	rs10529326	1	165,719,351	ATCTT	A	-0.077	0.017	1.2×10 <sup>-5</sup>	9
POAG	<i>MYOC</i>	rs12129856	1	171,580,024	A	G	0.051	0.015	6.6×10 <sup>-4</sup>	OMIM #601652
POAG	<i>CYP11B1</i>	rs2432663	2	38,351,642	T	C	0.096	0.027	4.5×10 <sup>-4</sup>	OMIM #231300
POAG	<i>FNDC3B</i>	rs199612704	3	172,033,011	G	C	0.164	0.040	3.9×10 <sup>-5</sup>	10, 39
POAG	<i>AFAP1</i>	rs4328916	4	7,823,5861	TATAC	T	0.044	0.011	5.9×10 <sup>-5</sup>	24
POAG	<i>GMDS</i>	rs182635870	6	2,345,598	G	T	0.481	0.126	1.4×10 <sup>-4</sup>	24
POAG	<i>8q22</i>	rs7009228	8	105,721,414	A	G	-0.051	0.012	2.0×10 <sup>-5</sup>	14
POAG	<i>9p21</i>	rs2383204	9	22,055,048	G	A	0.048	0.011	2.3×10 <sup>-5</sup>	9, 24
POAG	<i>9p21</i>	rs79721419	9	22,200,956	A	G	0.141	0.035	6.6×10 <sup>-5</sup>	this study
POAG	<i>ABO</i>	rs551169	9	136,197,286	A	G	0.047	0.011	1.1×10 <sup>-5</sup>	39
advanced	<i>PMM2</i>	rs13332985	16	8,908,857	A	G	-0.049	0.013	4.1×10 <sup>-4</sup>	11
advanced	<i>GAS7</i>	rs8080535	17	9,968,097	G	A	-0.044	0.011	1.3×10 <sup>-4</sup>	54

Sample size was 1875 cases and 1709 controls for POAG and 946 cases and 1709 controls for advanced POAG. For this table the “best phenotype,” the phenotype with the greatest significance of association, is reported.

Correction for multiple testing is 0.05 / (2 phenotypes times 25 candidate genes) = 0.001. Uncorrected p-values are given.

SNPs listed have p value < 0.001, MAF > 0.005, and imputation quality > 0.70, one result per locus shown.

The following 25 loci were tested: *8q22*<sup>14</sup>, *9p21*<sup>7, 8, 14</sup>, *ABCA1*<sup>11, 24</sup>, *ABO*<sup>39</sup>, *AFAP1*<sup>40</sup>, *ARHGGEF12*<sup>41</sup>, *ATOH7*<sup>42</sup>, *ATXN2*<sup>6, 22</sup>, *CAVI*<sup>23, 43</sup>, *CYP11B1* (OMIM#231300), *FNDC3B*<sup>10</sup>, *GAS7*<sup>22</sup>, *FOXC1/GMDS*<sup>15, 22</sup>, *LTBP2* (OMIM#613086)<sup>13</sup>, *MIR182*<sup>26</sup>, *MYOC* (OMIM#601652)<sup>7</sup>, *OPTN* (OMIM#137760), *PMM2*<sup>11</sup>, *SIX1/SIX6*<sup>25</sup>, *TBK1* (OMIM#177700), *TGFBR3*<sup>10</sup>, *TMCO1*<sup>9</sup>, *TXNRD2*<sup>22</sup>.

Combined logistic regression of 11 SNPs and POAG

	Estimate	Standard Error	p value
Intercept	-0.833	0.334	0.0126
African continental ancestry	0.432	0.250	0.0838
rs10529326	<i>TMCO1</i>	0.364	0.073
rs2432663	<i>CYP11B1</i>	0.476	0.119
rs199612704	<i>FNDCC3B</i>	0.818	0.163
rs4328916	<i>AFAP1</i>	0.197	0.048
rs7009228	<i>8q22</i>	0.259	0.051
rs2383204	<i>9p21#1</i>	0.232	0.051
rs79721419	<i>9p21#2</i>	0.616	0.151
rs551169	<i>ABO</i>	0.196	0.046
rs8080535	<i>GAS7</i>	0.159	0.047
rs235902	<i>MYOC</i>	0.174	0.067
rs1332985	<i>PMM2</i>	0.104	0.053

The genotypes of those SNPs in Table 1 with negative effect sizes were re-coded to the other allele so that the number of alleles for each SNP was additive for increased POAG risk. All SNPs were then combined into a single logistic regression model. AD for each subject was estimated using Admixture 1.3.0 with  $K=3$  on a subset of the genotyping data pruned for linkage disequilibrium. The dataset for this table, with genotypes coded to be additive, was then used to create Genetic Risk Score #1. Note that both *9p21* SNPs, rs2383204 and rs79721419, remained in this model, further supporting their statistical independence.

Table 2.

**Table 3.**

## Summary of Findings

Gene	SNP in this report	Phenotype	Relationship(s) to previously reported SNPs for POAG
<i>TGFBR3</i>	rs11466588	POAG	No LD with prior rs2810903.
<i>TMCO1</i>	rs10529326	POAG	In LD with prior rs4656461 and prior rs7518099. <sup>9</sup>
<i>MYOC</i>	rs12129856	POAG	No association observed with previously published SNPs. SNP is located in adjacent gene, <i>PRRC2C</i> . (Fig. 4)
<i>CYP11B1</i>	rs2432663	POAG	rs2432663 is located between <i>CYP11B1</i> and <i>CYP11B1-AS1</i> .
<i>FNDC3B</i>	rs199612704	POAG	No LD with prior rs12897; separated by region of high recombination (Fig. 3A&B).
<i>AFAP1</i>	rs4328916	POAG	No LD with prior rs4619890. <sup>24</sup>
<i>8q22</i>	rs7009228	POAG	No LD with previously reported rs1521444, rs284489, or rs284495. <sup>14</sup> Closer to <i>LRP12</i> gene.
<i>9p21</i>	rs2383204, rs79721419	POAG	Two independent signals identified. Signal #1 at rs2383204 is in linkage disequilibrium with previously published SNPs rs1063192 <sup>42</sup> and rs4977756. <sup>9</sup> Signal #2 at rs79721419 is approximately 150kb away from #1 and separated by a region of high recombination (Fig. 2)
<i>ENO4</i>	rs185815146	Advanced POAG	Putative novel locus for AD POAG
<i>ABO</i>	rs551169	POAG	No LD with prior rs8176743; located in <i>ABO</i> promoter. <sup>39</sup>
<i>PMM2</i>	rs13332985	Advanced POAG	No LD with prior rs3785176 or rs8057024. <sup>11</sup>
<i>GAS7</i>	rs8080535	Advanced POAG	No LD with prior rs12150284; separated by region of high recombination (Fig. 3C&D). <sup>54</sup>

Note: Linkage disequilibrium (LD) between SNPs was assessed using the “AMR” subset of the 1kGP data. This set will contain genomic segments from African, Amerindian, European ancestry. “Prior” indicates SNPs reported to be genome-wide significant in a genome-wide association study.